https://doi.org/10.18502/jad.v20i2.22399

Original Article

Integrating Local Occurrence Records and Monthly Spatiotemporal Thermal Analysis to Predict Current and Future High-Risk Areas of *Aedes albopictus* in Guilan Province, Iran

Samira Karimi[1,2,3], *Ensiyeh Jamshidi[3,4], Masud Yunesian[1,5], Shahyad Azari-Hamidian[6,7], Behzad Norouzi[6], Morteza Pourgholami[8], *Ahmad Ali Hanafi-Bojd[2,9]

[1]Department of Environmental Health Engineering, School of Public Health, Tehran University of Medical Sciences, Tehran, Iran
[2]Zoonoses Research Center, Tehran University of Medical Sciences, Tehran, Iran
[3]Student's Scientific Research Center, Tehran University of Medical Sciences, Tehran, Iran
[4]Department of Health Education and Promotion, School of Public Health, Tehran University of Medical Sciences, Tehran, Iran
[5]Center for Air Pollution Research, Institute for Environmental Research, Tehran University of Medical Sciences, Tehran, Iran
[6]Research Center of Health and Environment, School of Health, Guilan University of Medical Sciences, Rasht, Iran
[7]Department of Medical Parasitology, Mycology and Entomology, School of Medicine, Guilan University of Medical Sciences, Rasht, Iran
[8]Vice-Chancellorship of Health, Guilan University of Medical Sciences, Rasht, Iran
[9]Department of Vector Biology and Control of Diseases, School of Public Health, Tehran University of Medical Sciences, Tehran, Iran

***Corresponding authors:** Dr Ahmad Ali Hanafi-Bojd, E-mail: aahanafibojd@tums.ac.ir; Dr Ensiyeh Jamshidi, E-mail: ensiyeh_jamshidi@yahoo.com

(Received 01 May 2026; accepted 27 June 2026)

Abstract

Background: *Aedes albopictus*, a key vector of arboviral diseases, has already been detected in Guilan Province, Iran, and is emerging as a public health concern in the country. This study aimed to identify monthly high-risk areas of *Ae. albopictus* and predict its distribution in Guilan Province using ecological niche modeling under current and projected climate scenarios. Guilan Province, with its high annual influx of travellers and active maritime ports, represents a strategic area for monitoring *Ae. albopictus* establishment.

Methods: A total of 200 occurrence points were obtained from local entomological surveys and health authorities. Four MaxEnt models were developed: current baseline (bioclimatic variables + elevation); current enhanced (bioclimatic variables + elevation + LST, NDVI, NDWI and population); and two future scenarios (SSP1-2.6 and SSP5-8.5, year 2030, CMIP6). Model performance was excellent, with AUC values of 0.909 and 0.908 for the baseline and enhanced models, respectively. Monthly thermal suitability maps were generated based on 2024 meteorological data using the optimal temperature range of 15–35 °C.

Results: Under the SSP5-8.5 scenario, risk areas expanded, and the monthly analysis indicated that nearly the entire Guilan Province exhibited suitable conditions for seven months of the year. The warm months showed the highest probability of *Ae. albopictus* presence across the province.

Conclusions: These findings provide critical insights for targeted vector surveillance and control strategies in the region.

Keywords: Asian tiger mosquito; Climate Change; Invasive mosquito; MaxEnt; Risk Mapping

Introduction

Aedes albopictus, commonly known as the Asian tiger mosquito, is a highly invasive species

http://jad.tums.ac.ir
Published Online: June 30, 2026

Copyright © 2026 The Authors. Published by Tehran University of Medical Sciences.
This work is licensed under a Creative Commons Attribution-NonCommercial 4.0 International license (https://creativecommons.org/licenses/by-nc/4.0/). Non-commercial uses of the work are permitted, provided the original work is properly cited.

https://doi.org/10.18502/jad.v20i2.22399

and one of the principal vectors of arboviral diseases, including dengue, chikungunya and Zika viruses (1). The rapid global expansion of *Ae. albopictus* has substantially increased the geographic risk of dengue transmission, underscoring the need for accurate ecological risk assessment and targeted vector surveillance (1). Globally, an estimated 390 million dengue infections occur annually, of which approximately 96 million are clinically apparent (2). In 2023, more than 5 million dengue cases and over 5,000 dengue-related deaths were reported across more than 80 countries, highlighting the growing global public health burden of the disease (3, 4).

In Iran, dengue fever has gradually shifted from imported cases to local transmission over the past two decades (5). In 2024, autochthonous dengue cases were reported in southern provinces, including Hormozgan and Sistan and Baluchestan, with a total of 221 confirmed cases (150 imported and 71 locally transmitted) (5). The establishment of *Aedes* vectors in both southern and northern regions of the country, together with favorable climatic conditions, has increased the potential for further dengue transmission (6, 7). In addition, challenges such as inadequate urban infrastructure and limited public and healthcare awareness complicate vector control efforts, emphasizing the need for strengthened surveillance and early risk assessment in environmentally suitable regions of Iran.

A regional ecological niche modeling study by Ducheyne et al. (8) predicted the current and future distribution of *Ae. aegypti* and *Ae. albopictus* across the WHO Eastern Mediterranean Region and identified environmentally suitable areas for the establishment of *Ae. albopictus* in Iran. However, the study was conducted at a broad regional scale and did not capture local environmental heterogeneity or seasonal variations in habitat suitability within individual provinces such as Guilan (8). These limitations highlight the need for local-scale studies using regional occurrence data to support more accurate vector surveillance and risk assessment.

Guilan Province, located in northern Iran, provides highly favorable ecological and climatic conditions for the establishment of invasive *Aedes* mosquitoes (9). The first record of *Ae. albopictus* in Guilan by Azari-Hamidian et al. (10) confirmed the establishment of this invasive species in the province and expanded the known mosquito fauna of northern Iran. Although no autochthonous dengue, chikungunya or Zika cases have been reported in Guilan to date, predictive modeling has consistently identified the province as one of the most environmentally suitable areas for *Ae. albopictus* establishment under both current and future climatic conditions (9). Favorable environmental characteristics, including suitable temperatures, high humidity and abundant breeding habitats, further support mosquito survival and proliferation (11). These findings suggest that Guilan represents a high-priority region for proactive vector surveillance and early risk assessment before local transmission becomes established.

Located along the Caspian Sea, Guilan Province is an important transportation, trade and tourism hub, with active maritime ports and substantial annual human mobility (12–14). These characteristics increase the likelihood of introducing dengue-infected travelers into the province. Given the established presence of *Ae. albopictus* and the ongoing circulation of dengue in southern Iran, Guilan represents a high-priority region for surveillance because the continuous movement of travelers may facilitate virus introduction. Therefore, continuous vector surveillance and early ecological risk assessment are essential for preventing future outbreaks.

Aedes albopictus develops within a temperature range of approximately 15–35 °C, with optimal development occurring between 25 and 30 °C (15, 16). Its life cycle, survival and seasonal activity are strongly influenced by temperature and photoperiod, resulting in pronounced temporal fluctuations in mosquito abundance. Consequently, evaluating habitat

http://jad.tums.ac.ir
Published Online: June 30, 2026

https://doi.org/10.18502/jad.v20i2.22399

suitability at a monthly rather than annual scale is essential for capturing seasonal changes in vector activity and identifying periods of increased transmission risk. Such information can support timely vector surveillance, targeted control interventions and early warning systems for mosquito-borne diseases (17).

Understanding the thermal limits of *Ae. albopictus* is essential for predicting its survival, development and potential establishment (18). Ecological niche modeling (ENM) has been widely applied to estimate species distributions based on environmental conditions, with the Maximum Entropy (MaxEnt) model being one of the most commonly used approaches for presence-only data (19, 20). In addition to bioclimatic variables and elevation, environmental indicators such as Land Surface Temperature (LST), Normalized Difference Vegetation Index (NDVI), Normalized Difference Water Index (NDWI) and human population density can improve habitat suitability predictions (21). LST directly influences mosquito development, survival and activity, whereas NDVI reflects vegetation cover that may provide favorable resting and humid microhabitats. NDWI serves as an indicator of water availability and potential breeding habitats, while population density represents the intensity of human–vector contact and the potential for mosquito establishment in human-dominated environments.

Future climate projections derived from CMIP6, including SSP1-2.6 and SSP5-8.5, provide a valuable framework for assessing how climate change may alter the future distribution of *Ae. albopictus* and identify areas at increased risk of establishment in northern Iran (22). However, most previous ecological niche modeling studies have relied on global occurrence datasets and annual climatic averages, providing limited information on local environmental heterogeneity and seasonal habitat dynamics, particularly in Guilan Province (9). Furthermore, no previous study has integrated local mosquito occurrence records with monthly temperature-based thermal suitability mapping to characterize the spatiotemporal dynamics of *Ae. albopictus* in this region. Given the absence of autochthonous dengue transmission in Guilan, such predictive analyses are essential for proactive surveillance and early risk assessment before local transmission occurs. Therefore, this study aimed to determine the monthly spatiotemporal patterns of *Ae. albopictus* habitat suitability in Guilan Province by integrating local temperature-based thermal mapping with MaxEnt species distribution modeling under current (2024) and near-future climate scenarios (2021–2040 climatological period; SSP1-2.6 and SSP5-8.5).

Materials and Methods

Study area

Guilan Province, located along the Caspian Sea in northern Iran, covers an area of 14,042 km² and features a humid subtropical climate (23). According to the 2016 national census, the total population of Guilan Province is approximately 2.53 million people (24). Based on the National Tourist Census, nearly 28–30 million tourists visit Guilan Province annually (25). Its strategic location, with active maritime ports and substantial travel and trade, makes it a key area for mosquito surveillance and vector control planning.

Occurrence data

A total of 200 adult *Ae. albopictus* occurrence records were obtained through the routine entomological surveillance program of the Guilan Provincial Health Authority during 2024 (26). Surveillance was conducted in urban, rural, forested and cemetery areas. Potential breeding sites were initially identified using ovitrap surveillance, after which adult mosquitoes were collected from ovitrap-positive locations. Adult specimens were morphologically identified using the identification keys of Azari-Hamidian and Harbach (27, 28). Geographic coordinates were recorded using smartphone GPS applications

http://jad.tums.ac.ir
Published Online: June 30, 2026

https://doi.org/10.18502/jad.v20i2.22399

with an accuracy of approximately 5–10 m. After removing one duplicate record with identical geographic coordinates using Microsoft Excel, 199 unique occurrence records remained for subsequent analyses. To reduce spatial sampling bias and minimize spatial autocorrelation, the occurrence points were screened using the SDM Toolbox 2.4 in ArcGIS 10.8 (29). A 1-km thinning distance was selected to match the spatial resolution of the environmental variables (~1 km). No additional records were removed during spatial thinning because all remaining occurrence points were separated by more than 1 km.

Environmental, climatic and human population data

For the current distribution models, nineteen bioclimatic variables (BIO1–BIO19) were obtained from the WorldClim database (version 2.1) representing the baseline climate period (1970–2000) at a spatial resolution of 30 arc-seconds (~1 km) (30). Pearson correlation analysis was performed in ArcGIS (Spatial Statistics Tools), and variables with correlation coefficients greater than 0.7 were excluded to minimize multicollinearity. Five ecologically relevant variables were retained: BIO1 (annual mean temperature), BIO3 (isothermality), BIO5 (maximum temperature of the warmest month), BIO12 (annual precipitation) and BIO15 (precipitation seasonality).

Elevation (ALT) was derived from the Shuttle Radar Topography Mission (SRTM) at a spatial resolution of 30 arc-seconds (~1 km) (30). Land Surface Temperature (LST), Normalized Difference Vegetation Index (NDVI) and Normalized Difference Water Index (NDWI) were derived from MODIS products using Google Earth Engine and processed into annual mean composites for 2024. Human population density was obtained from the WorldPop database (2020) and resampled to match the environmental layers (31). The use of datasets from different years reflects the most recent publicly available data for each variable and is not expected to substantially affect the broad-scale habitat suitability analysis.

All environmental layers were clipped to the administrative boundary of Guilan Province, converted to ASCII raster (asc) format, and aligned to a common spatial extent for MaxEnt analysis.

For future projections, downscaled CMIP6 climate data from the MIROC6 global climate model were obtained from WorldClim version 2.1 for the 2021–2040 climatological period, representing near-term climatic conditions centered around 2030. Two Shared Socioeconomic Pathways (SSP1-2.6 and SSP5-8.5) were used. Only the selected bioclimatic variables and elevation were included in the future models, whereas LST, NDVI, NDWI and population density were not projected and therefore were not incorporated into future predictions.

Ecological niche modeling

Species distribution modeling was performed using MaxEnt version 3.4.4. Four models were developed:

Current baseline model: using bioclimatic variables and elevation.

Current enhanced model: using bioclimatic variables, elevation, LST, NDVI, NDWI and human population density.

Future model (SSP1-2.6): using bioclimatic variables and elevation.

Future model (SSP5-8.5): using bioclimatic variables and elevation.

Feature types were set to Auto, and the regularization multiplier was set to 1 (default). Ten replicate runs were performed using cross-validation with 80% of occurrence records used for training and 20% for testing. Model outputs were generated in logistic format, providing habitat suitability values ranging from 0 (unsuitable) to 1 (highly suitable).

Model performance was evaluated using the area under the receiver operating characteristic curve (AUC) and gain values. Environmental variable importance was assessed using percent contribution, permutation importance and Jackknife tests.

http://jad.tums.ac.ir
Published Online: June 30, 2026

https://doi.org/10.18502/jad.v20i2.22399

Monthly thermal suitability analysis

Monthly minimum, mean and maximum air temperature data from 28 meteorological stations across Guilan Province for 2024 were obtained from the Guilan Meteorological Organization. A thermal suitability threshold of 15–35 °C was applied based on published biological requirements of adult *Ae. albopictus* (15, 16). Monthly thermal suitability maps were generated using the Inverse Distance Weighting (IDW) interpolation method in ArcGIS with a power parameter of 2.

Mapping and visualization

All raster layers and model outputs were processed and visualized in ArcGIS version 10.8. Monthly thermal suitability maps and present and future potential habitat suitability maps under the SSP scenarios were generated for Guilan Province. For visualization purposes, continuous habitat suitability values produced by MaxEnt (0–1) were classified into five classes: very low (0–0.20), low (0.20–0.40), moderate (0.40–0.60), high (0.60–0.80) and very high (0.80–1.00). The classification was used only for map display and interpretation.

Results

Model performance

The predictive performance of the MaxEnt models was evaluated using the average test Area Under the Receiver Operating Characteristic Curve (AUC) and standard deviation (SD) across 10 replicate runs (Table 1). The mean test AUC values were 0.909±0.012 for the current baseline model, 0.908±0.019 for the current enhanced model and 0.909±0.012 for both future scenarios (SSP1-2.6 and SSP5-8.5), indicating consistently good predictive performance across all models. Although the enhanced model included additional environmental variables, its average test AUC was comparable to that of the baseline model, indicating that the additional predictors did not substantially alter the overall discriminatory performance of the model but provided additional environmental information for characterizing habitat suitability.

Jackknife tests of variable importance were performed for each model using both regularized training gain and test gain (Figs. 1 and 2). The Jackknife results represent the relative importance of predictor variables within the MaxEnt modeling framework and should therefore be interpreted as indicators of their relative contribution to model performance rather than as direct evidence of ecological causality.

For the current baseline model, altitude (ALT) produced the highest gain when used in isolation (blue bars; training gain ≈ 1.1, test gain ≈ 1.1), indicating that it contained the greatest amount of unique information among the predictor variables. Conversely, omission of altitude from the model (green bars) substantially reduced model gain (training gain ≈ 0.55, test gain ≈ 0.55), indicating that this variable made a strong contribution to model performance. Other climatic variables, including BIO1 (annual mean temperature), BIO12 (annual precipitation) and BIO15 (precipitation seasonality), also contributed to model performance.

When all predictor variables were included simultaneously (red bars), the highest training (≈1.5) and test gain (≈1.45) values were obtained, indicating that the combined set of environmental variables provided the greatest predictive information for habitat suitability.

For the current enhanced model, population density showed the highest individual training gain when used alone (blue bar ≈ 1), indicating that it provided the greatest amount of unique information among the variables included in this model. Removal of population density (green bar) resulted in a noticeable reduction in model gain, suggesting an important contribution within the modeling framework. Similar patterns were observed for the test gain. However, according to the percent contribution analysis (Table 3), LST was the dom-

http://jad.tums.ac.ir
Published Online: June 30, 2026

https://doi.org/10.18502/jad.v20i2.22399

inant predictor (59.9%), indicating that while population density contributed the greatest unique information in the Jackknife analysis, LST contributed most to the overall model fitting. BIO5, BIO3, NDWI and elevation also showed relatively high gains when evaluated individually.

The Jackknife results for the future SSP1-2.6 model showed that elevation produced the highest training gain when used alone (blue bar ≈ 1.05), indicating that it contained the highest amount of unique predictive information under this climate scenario. Removal of annual mean temperature (BIO1) and annual precipitation (BIO12) also reduced model gain, indicating that these variables contributed to the final model. BIO3, BIO15 and BIO5 provided additional predictive information but had smaller effects than elevation. The test gain showed a similar pattern, with elevation remaining the strongest predictor within the model. When elevation was omitted, test gain declined markedly, indicating its strong contribution to model performance.

Similarly, for the SSP5-8.5 model, elevation yielded the highest training and test gain values, while omission of elevation resulted in the largest reduction in model gain. Annual precipitation (BIO12), precipitation seasonality (BIO15) and maximum temperature of the warmest month (BIO5) also contributed to the model, whereas annual mean temperature (BIO1) and isothermality (BIO3) provided comparatively lower individual gains.

Variable contribution and importance

The relative percent contribution and permutation importance of environmental variables are presented in Tables 2 and 3. For the current baseline model and both future scenarios (SSP1-2.6 and SSP5-8.5), altitude showed the highest percent contribution (70.7%), followed by BIO12 (9.0%). Other variables contributed to the model to a lesser extent but also influenced habitat suitability. Altitude also exhibited the highest permutation importance (60.3%), followed by BIO12 (11.2%) and BIO1 (10.3%). This pattern was consistent across the current baseline and both future models, indicating similar relative importance of predictor variables under current and projected climatic conditions (Table 2).

For the current enhanced model, LST showed the highest percent contribution (59.9%), followed by BIO12 (10.7%) (Table 3). Land Surface Temperature also exhibited the highest permutation importance (25.1%), followed by population density (16.7%) and elevation (16.0 %). Consistent with the Jackknife analysis, these results indicate that LST was the dominant predictor during model fitting, whereas population density provided substantial unique information to the model when evaluated independently. Together, these findings suggest that LST and population density were influential predictors of habitat suitability within the MaxEnt modeling framework.

Response curves

The marginal response curves of the most influential variables in each model illustrate how predicted habitat suitability changes while all other variables are held constant (Fig. 3). Elevation showed the highest contribution in the current baseline model as well as in the SSP1-2.6 and SSP5-8.5 future models. The response curves indicated that habitat suitability was highest at low elevations, particularly near sea level, and declined progressively with increasing altitude. Suitability decreased sharply above approximately 400–500 m, suggesting that *Ae. albopictus* is primarily associated with lowland and coastal environments that provide favorable climatic conditions for survival and breeding. This pattern is consistent with the ecological characteristics of the species, which is typically restricted to low-elevation areas in temperate regions.

In the current enhanced model, LST was the most influential predictor according to percent contribution. The response curve showed that habitat suitability reached its maximum at approximately 20–25 °C and declined progressively at higher land surface temperatures. This

http://jad.tums.ac.ir
Published Online: June 30, 2026

https://doi.org/10.18502/jad.v20i2.22399

pattern suggests that *Ae. albopictus* is associated with relatively moderate land surface temperatures, whereas excessively high temperatures may reduce habitat suitability by limiting survival, egg viability and breeding activity. These findings are consistent with previous studies reporting that *Ae. albopictus* thrives under mild thermal conditions and is less likely to persist in areas with very high land surface temperatures.

Spatiotemporal analysis of thermal suitability for *Aedes albopictus* activity across different months

Monthly minimum, mean and maximum air temperature data from 28 meteorological stations across Guilan Province for 2024 were used to generate monthly thermal suitability maps for *Ae. albopictus* (Fig. 4). A thermal suitability threshold of 15–35 °C was applied based on published biological requirements of adult *Ae. albopictus*. Temperature surfaces were interpolated using the Inverse Distance Weighting (IDW) method in ArcGIS.

The resulting maps show thermal suitability across the 12 months of the year in Guilan Province, from January to December. Areas with mean temperatures within the thermal suitability threshold (15–35 °C) are highlighted in red, cooler areas (<15 °C) are shown in blue, and areas exceeding 35 °C are shown in yellow.

The classified thermal maps for January, February and March indicate that all areas of Guilan Province fall within the temperature category below 15 °C. These regions, depicted in blue on the maps, represent unfavorable thermal conditions for adult *Ae. albopictus* activity.

Because monthly mean temperatures remained below the lower thermal threshold (15 °C), adult mosquito activity was expected to be very limited during these months, although the persistence of diapausing eggs cannot be excluded.

The classified thermal map for April shows that most lowland and central areas of Guilan Province fall within the temperature range of 15–35 °C, depicted in red on the maps. This pattern indicates the beginning of the seasonal expansion of thermally suitable conditions for *Ae. albopictus*, particularly in lowland areas such as Rasht, Bandar-e-Anzali, Somehsara, Astaneh Ashrafiyeh, Lahijan and the coastal areas of Talesh.

However, some mountainous and higher-altitude regions remain below 15 °C, shown in blue. These areas include parts of Rudsar, Siyahkal (Deylaman) and the highlands of Fooman and Rezvanshahr, where temperatures remain below the thermal suitability threshold.

Overall, April represents the onset of widespread thermally suitable conditions across the lowland areas of the province, with further expansion expected as temperatures increase.

The classified thermal map for May shows that nearly the entire Guilan Province falls within the 15–35 °C range, depicted in red. This indicates that thermally suitable conditions for adult *Ae. albopictus* had expanded across almost the entire province. Only a few small and scattered mountainous areas in Rezvanshahr, Fooman, Shaft, Rudbar and Siyahkal remained below 15 °C because of their higher elevations.

The classified thermal maps for June, July, August and September show that almost the entire province remained within the 15–35 °C thermal suitability range. During these months, thermally suitable conditions extended across both lowland and most mountainous regions of Guilan Province.

The highest spatial extent of thermally suitable conditions was observed during July–September, when nearly the entire province fell within the defined thermal suitability range. Only limited high-altitude areas of Rezvanshahr remained below the threshold in September.

In October, the spatial pattern was similar to that observed in April, with most lowland and central areas remaining within the 15–35 °C range, whereas mountainous areas of Rudsar, Siyahkal (Deylaman), Fooman, Rezvanshahr and some elevated areas between Rasht and Somehsara remained below the lower threshold.

In November, most areas of the province fell below the thermal suitability threshold, with only a limited area in the highlands of Rudbar remaining within the 15–35 °C range.

http://jad.tums.ac.ir
Published Online: June 30, 2026

https://doi.org/10.18502/jad.v20i2.22399

The classified thermal map for December showed that all areas of Guilan Province fell below 15 °C, representing unfavorable thermal conditions for adult *Ae. albopictus* activity.

Overall, the thermal suitability maps indicated that favorable temperature conditions for adult *Ae. albopictus* were primarily restricted to the period from April to October, with the broadest spatial extent occurring during the summer months. These monthly thermal suitability maps were interpreted together with the MaxEnt habitat suitability maps to identify areas and periods where suitable environmental conditions coincided with favorable thermal conditions for the species.

Predicted distributions

The predicted current and future habitat suitability of *Ae. albopictus* was mapped to visualize areas with varying levels of habitat suitability (Fig. 5). For visualization purposes, habitat suitability values were classified into five classes: very low (0–0.20), low (0.20–0.40), moderate (0.40–0.60), high (0.60–0.80) and very high (0.80–1.00), represented by a color gradient from green to red.

According to the current baseline MaxEnt model, areas of high suitability were concentrated in Bandar-e-Anzali, Rasht and a small area along the border of Astara. Moderate suitability was observed in Somehsara, whereas low suitability occurred in the high-altitude and cooler mountainous regions. These results suggest that lowland and coastal regions provide the most favorable environmental conditions for habitat suitability of *Ae. albopictus* under current climatic conditions.

The current enhanced model, which incorporated additional environmental variables including LST, NDVI and population density, showed hotspots of high suitability primarily concentrated in Bandar-e-Anzali, Rasht and a small area along the border of Astara. Compared with the baseline model, the enhanced model identified a slightly expanded area of suitable habitat in Astara. Low suitability persisted in mountainous regions such as Rudbar, Rudsar and Masal, consistent with temperature and elevation constraints.

Under the SSP1-2.6 scenario, areas of high suitability were primarily located in Bandar-e-Anzali, Rasht, Somehsara, Lahijan and border areas of Astara, Talesh and Rezvanshahr. Low suitability remained in mountainous regions such as Rudbar, Rudsar, and Masal.

The SSP5-8.5 scenario showed a spatial pattern largely similar to that of SSP1-2.6, with only a slight expansion of highly suitable habitats in the central part of Guilan Province.

Table 1. Model evaluation metrics (AUC and standard deviation) for MaxEnt models of *Aedes albopictus* distribution under current conditions (2024) and future climate scenarios (2021–2040 climatological period) in Guilan Province, Iran

Model	AUC	Standard deviation
Current baseline	0.909	0.012
Current enhanced	0.908	0.019
SSP1-2.6	0.909	0.012
SSP5-8.5	0.909	0.012

Table 2. Variable contribution and permutation importance for the current (2024) model and future SSP1-2.6 / SSP5-8.5 (2021–2040 climatological period) MaxEnt models predicting the distribution of *Aedes albopictus* in Guilan Province, Iran

Variable	Percent contribution	Permutation importance
Altitude	70.7	60.3
Bio12	9	11.2
Bio15	7.5	7.1
Bio5	6.8	10.2
Bio1	3.3	10.3
Bio3	2.7	1

http://jad.tums.ac.ir
Published Online: June 30, 2026

https://doi.org/10.18502/jad.v20i2.22399

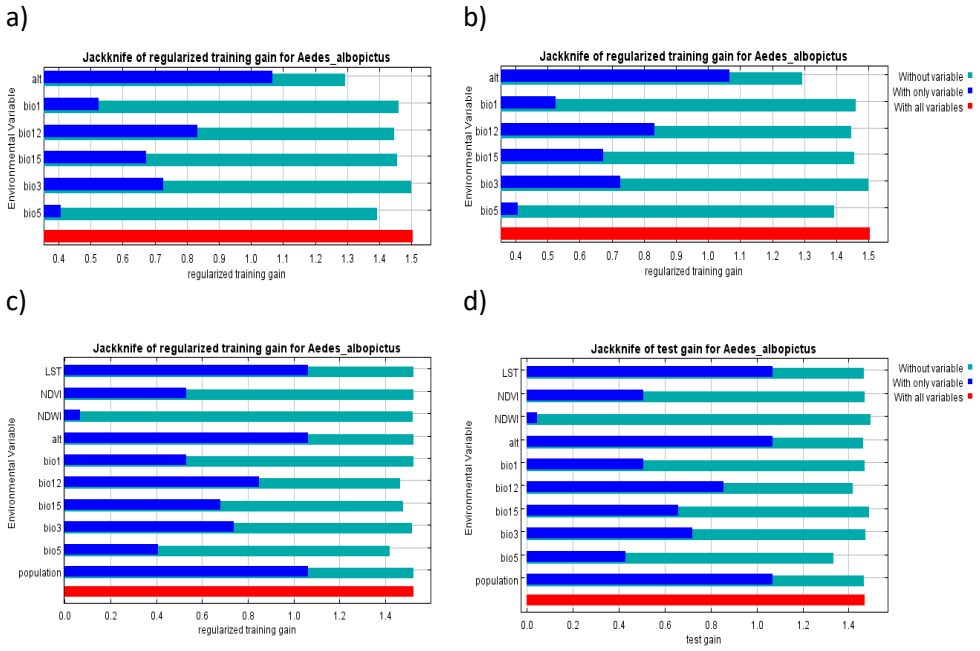


Fig. 1. Jackknife test of variable importance for the MaxEnt models of *Aedes albopictus*. Panels (a) and (b) show the contribution of environmental variables in the current baseline model, with (a) representing regularized training gain and (b) test gain. Panels (c) and (d) show the same for the current enhanced model, with (c) representing training gain and (d) test gain. All analyses were performed to model the present (2024) probability of presence of *Ae. albopictus* in Guilan Province, Iran, under current climatic conditions

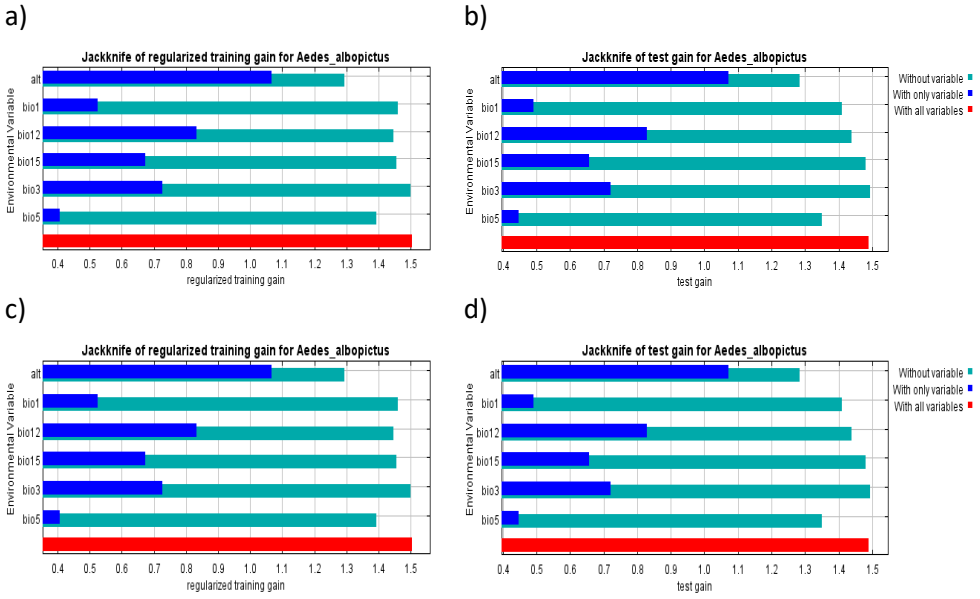


Fig. 2. Jackknife test of variable importance for the future SSP1-2.6 and SSP5-8.5 model (2030) of *Aedes albopictus*. Panels (a) and (b) show the contribution of environmental variables for the future SSP1-2.6 (2021–2040 climatological period) model, with (a) representing regularized training gain and (b) test gain. Panels (c) and (d) show the same for the future SSP5-8.5 model (2030), with (c) training gain and (d) test gain. All analyses were conducted to predict the future (2021–2040 climatological period) distribution of *Ae. albopictus* in Guilan Province, Iran

https://doi.org/10.18502/jad.v20i2.22399

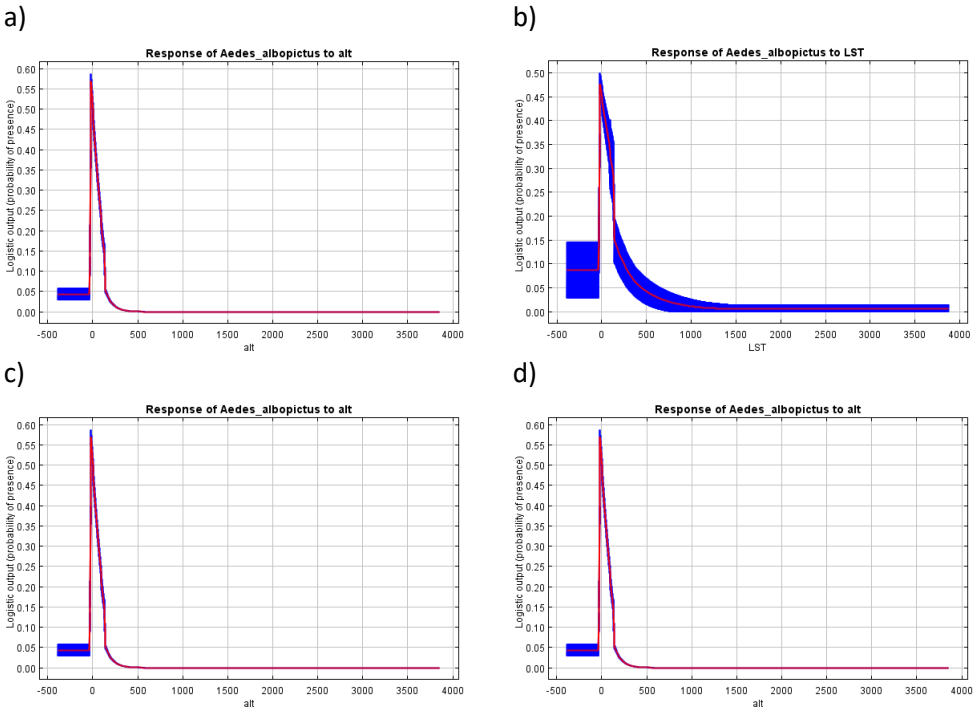


Fig. 3. Response curves of the most important environmental variables for *Aedes albopictus*. Panels (a, c, and d) show the response to elevation under the current baseline (2024) model and future scenarios SSP1-2.6 and SSP5-8.5 (2021–2040 climatological period), while panel (b) shows the response to Land Surface Temperature (LST) under the current enhanced (2024) model in Guilan Province, Iran

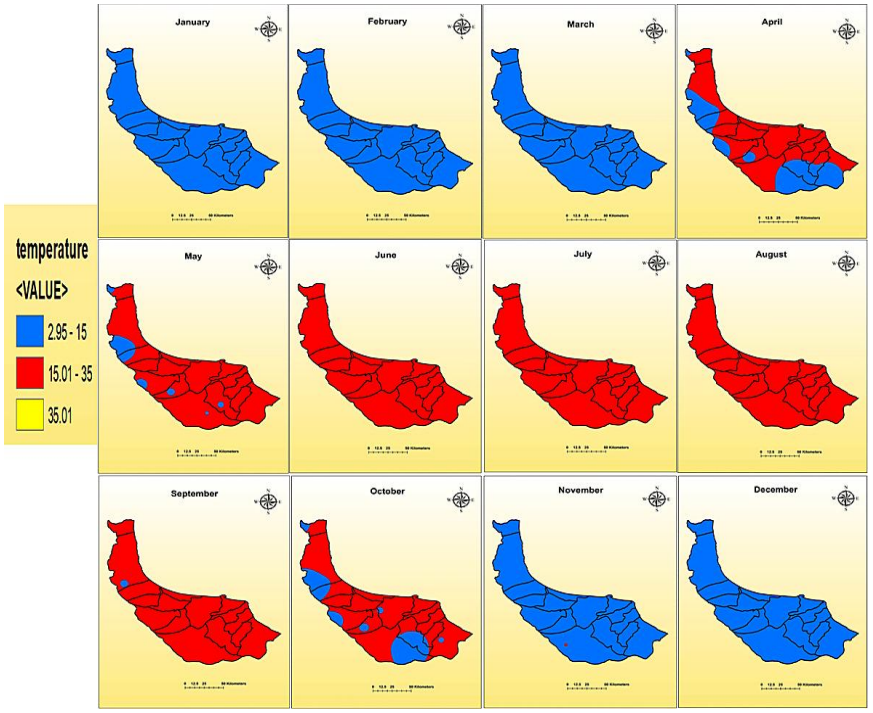


Fig. 4. Monthly thermal suitability maps for *Aedes albopictus* activity in Guilan Province based on 2024 mean temperatures (°C)

https://doi.org/10.18502/jad.v20i2.22399

Table 3. Variable contribution and permutation importance for the current enhanced (2024) MaxEnt model predicting the distribution of *Aedes albopictus* in Guilan Province, Iran

Variable	Percent contribution	Permutation importance
LST	59.9	25.1
Bio12	10.7	13.1
Bio15	7.5	10.3
Bio5	7.3	9.6
NDVI	4.9	5.8
Bio3	3.3	1.2
Population	2.5	16.7
Alt	2.3	16
Bio1	1	1.9
NDWI	0.6	0.4

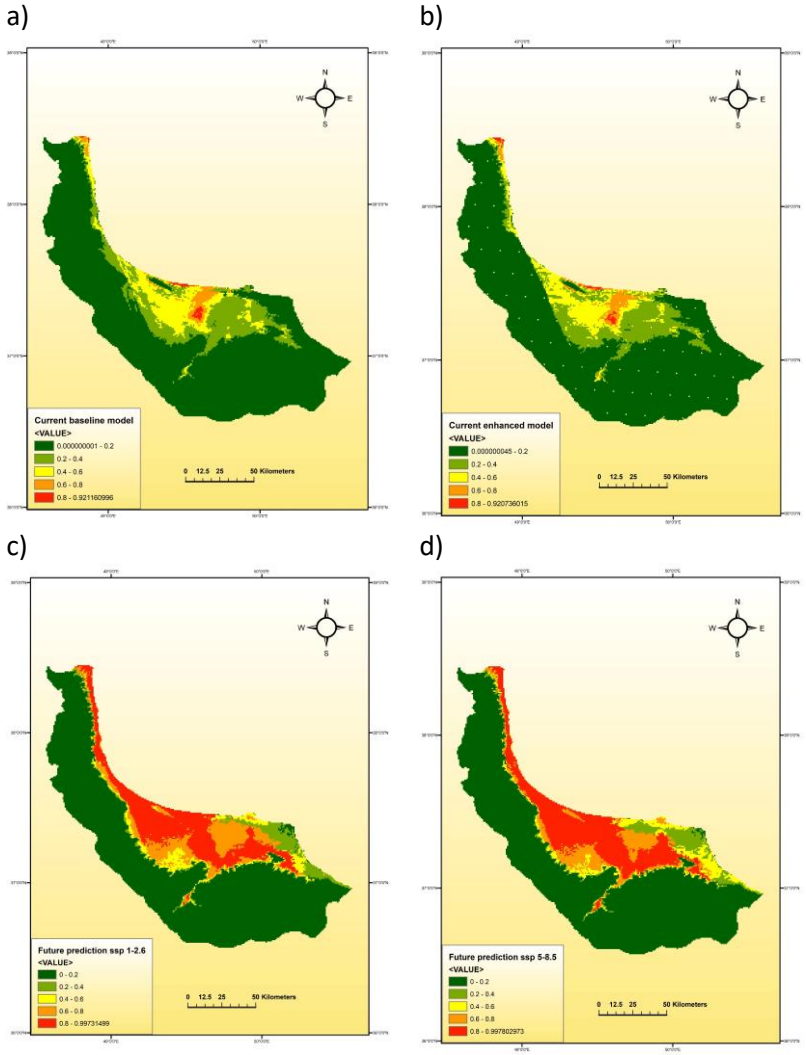


Fig. 5. Predicted current and future distributions of *Aedes albopictus* in Guilan Province under different scenarios. Panels show: (a) current baseline model (2024), (b) current enhanced model (2024) incorporating remote sensing and demographic variables, (c) future projection under SSP1-2.6 (2021–2040 climatological period), and (d) future projection under SSP5-8.5 (2021–2040 climatological period)

https://doi.org/10.18502/jad.v20i2.22399

Discussion

The present study provides an in-depth assessment of the environmental determinants and spatial distribution patterns of *Ae. albopictus* in Guilan Province, northern Iran, under current and future climatic conditions. By integrating climatic, remote sensing and demographic variables, this research offers a refined understanding of how local-scale factors shape the ecological niche of *Ae. albopictus* and how potential habitat suitability may evolve under different climate change scenarios.

The spatial modeling results revealed that *Ae. albopictus* is most likely to occur in the central and western parts of Guilan Province, particularly in Rasht, Bandar-e-Anzali and Astara. These areas share low elevations, high humidity and dense vegetation, which together create ideal conditions for larval development and adult survival. Future projections for representing the 2021–2040 climatological period (centered around 2030) under both SSP1-2.6 and SSP5-8.5 scenarios suggested a slight expansion of suitable habitats toward parts of the central and southern areas of the province while maintaining high suitability across the coastal zone. These results are consistent with Sedaghat et al. (9), who predicted high suitability for *Ae. albopictus* in the same regions based on national-scale modelling. However, the present study improves upon that work by using 199 field-confirmed occurrence points and high-resolution, locally calibrated environmental layers, resulting in an improved local-scale representation of the mosquito's distribution in Guilan.

Consistent with other studies, temperature, precipitation and vegetation cover emerged as dominant predictors of mosquito distribution (32, 33). However, the present model highlights that, at a local scale, additional variables such as land surface temperature (LST), vegetation index (NDVI), water index (NDWI) and human population density contribute to improving habitat characterization. These variables capture micro-environmental heterogeneity associated with urban heat, vegetation density, and breeding site availability that are often overlooked in coarse-resolution national or global datasets.

The comparison between the baseline and enhanced models further emphasizes this point. In the baseline model, which relied solely on climatic variables, elevation accounted for 70.7% of the total contribution, reflecting the strong dependence of mosquito occurrence on topographic and macroclimatic gradients. In contrast, when remote sensing and demographic variables were incorporated, LST became the most influential predictor in terms of percent contribution (59.9%), whereas population density showed high importance in the Jackknife analysis. These findings highlight the complementary value of microclimatic and anthropogenic variables in improving local-scale habitat characterization. Similar studies have likewise emphasized the importance of land surface temperature and human population in explaining the local distribution of *Aedes* mosquitoes, particularly in urbanizing environments (34–36).

In interpreting the response curves, the dominant influence of elevation and LST on the habitat suitability of *Ae. albopictus* reinforces the importance of both macro- and micro-environmental factors. The steep decline in predicted suitability above approximately 400–500 m elevation underscores the species' strong affinity for low-lying, humid coastal zones, consistent with previous findings showing that water-filled containers and dense vegetation in low-elevation environments favor larval development and adult survival (37). Likewise, the peak suitability observed at moderate surface temperatures (approximately 20–25 °C) and the subsequent decline at higher LST values indicate a thermal optimum beyond which habitat suitability decreases. This finding agrees with studies demonstrating that micro-scale tem-

http://jad.tums.ac.ir
Published Online: June 30, 2026

https://doi.org/10.18502/jad.v20i2.22399

perature variability, including urban heat island effects, significantly influences mosquito abundance and vectorial capacity (38).

Model performance metrics demonstrated good predictive accuracy for both current models (AUC ≈ 0.91). In the enhanced model, Jackknife analysis identified population density as one of the most influential variables, whereas LST showed the highest percent contribution. Together, these variables improved model performance by capturing local environmental heterogeneity that is not represented by climatic variables alone. These findings further support the importance of integrating socio-environmental factors into ecological niche models for reliable local-scale habitat prediction (39, 40).

A comparison of current and future scenarios further reveals meaningful trends. In the baseline and future climate models, elevation remained the most influential predictor, with a contribution exceeding 70%, reaffirming the species' preference for low-lying, humid and coastal environments. Temperature and precipitation variables also maintained their importance, although under future scenarios, particularly SSP5-8.5, the relative contributions of annual mean temperature (Bio1) and maximum temperature of the warmest month (Bio5) increased. This pattern is consistent with climate change projections suggesting that increasing temperatures may facilitate the expansion of environmentally suitable areas for *Ae. albopictus* (41, 42). Meanwhile, isothermality (Bio3) consistently exhibited low importance, indicating that the species responds more strongly to absolute temperature and precipitation than to seasonal temperature variability.

Jackknife tests for the future climate models further reaffirmed the importance of elevation, as excluding this variable produced the greatest reduction in model gain. At the same time, temperature-related variables contributed more strongly under warmer climate scenarios, suggesting that future warming may further enhance environmental suitability for *Ae. albopictus* establishment in parts of Guilan Province. Overall, the baseline and future projections consistently indicate that the coastal and central regions of Guilan will remain environmentally suitable for this invasive mosquito, supporting the need for continued vector surveillance and control.

The monthly distribution analysis adds an important temporal dimension to these findings. The monthly thermal suitability analysis indicated that thermally suitable conditions for adult *Ae. albopictus* occurred primarily from April to October, suggesting that adult activity is most likely during this period. Habitat suitability peaked between July and September, coinciding with the warm and humid summer months. These results are consistent with previous studies reporting that *Ae. albopictus* requires temperatures above approximately 15 °C to maintain sustained activity and successful breeding (16, 43). Conversely, during colder months (December–February), when temperatures fall below this threshold, the model predicted negligible suitability, corresponding to near dormancy of the species. These seasonal patterns confirm the temperature thresholds constraining *Ae. albopictus* survival and delineate the seasonal window of increased vector activity and potential vector establishment within the province.

High-altitude and mountainous regions, including Fooman, Rezvanshahr, Deylaman and parts of Talesh, consistently exhibited delayed suitability for *Ae. albopictus* activity because of lower temperatures. These findings agree with the Köppen climatic sub-classification of Guilan Province, where lowland areas correspond to the humid temperate (Cf) climate that supports earlier seasonal mosquito activity, whereas mountainous areas correspond to the cooler humid temperate (Cs) climate with shorter periods of environmental suitability (44). This distinction highlights the importance of tailoring vector surveillance and control strategies according to both elevation and local climatic conditions.

Despite its contributions, this study has several limitations. First, MaxEnt relies on pres-

http://jad.tums.ac.ir
Published Online: June 30, 2026

https://doi.org/10.18502/jad.v20i2.22399

ence-only records that may be influenced by sampling bias. Although 199 occurrence points were used, sampling was not completely randomized, and remote areas may have been underrepresented. Second, although multiple environmental and anthropogenic variables were incorporated, the cross-sectional nature of the analysis limits ecological interpretation regarding the relationships between environmental factors and mosquito distribution. Finally, because high-resolution local climate datasets were unavailable, global climate and satellite-derived datasets were used, which may introduce uncertainty into fine-scale predictions. Nevertheless, combining field-confirmed occurrence records, remote sensing products and future climate projections enhances the robustness of the modelling framework. In addition, future habitat suitability projections were based on a single global climate model (MIROC6) under two CMIP6 scenarios (SSP1-2.6 and SSP5-8.5). Although this approach is widely used, projections from different climate models may vary, and future studies incorporating multiple climate models could provide a more comprehensive assessment of projection uncertainty.

This study has several important strengths. It represents the first comprehensive local-scale ecological niche model of *Ae. albopictus* in Guilan Province integrating climatic, remote sensing, and demographic variables. In addition, this is the first study to integrate monthly thermal suitability mapping with MaxEnt-based ecological niche modeling for *Ae. albopictus* in Guilan Province. While broad climatic variables remained important, incorporating microclimatic and demographic information substantially altered the relative importance of predictors. In the enhanced model, LST showed the highest percent contribution (59.9%), emphasizing the importance of local environmental conditions for explaining mosquito habitat suitability. Furthermore, the monthly thermal suitability analysis provides practical information for seasonal surveillance and vector management. Such integrated modelling approaches offer valuable support for evidence-based public health planning and for anticipating vector establishment under changing climatic conditions.

Overall, the findings indicate that Guilan Province will remain environmentally suitable for *Ae. albopictus* under future climate scenarios. These results provide a scientific basis for strengthening vector surveillance, environmental monitoring and evidence-based planning for invasive mosquito management in northern Iran.

Conclusion

Guilan Province provides conducive environmental conditions for the establishment of *Ae. albopictus*, particularly in its coastal and central regions. Projected climate change is expected to expand the species' potential range and prolong its seasonal activity, elevating the risk of dengue transmission. These findings underscore the urgent need for continuous environmental surveillance, targeted vector control and adaptive public health strategies. Integrating climatic, demographic and remote sensing data offers a robust framework for evidence-based planning and proactive management of vector-borne disease risks under changing environmental conditions.

Acknowledgements

The project was financially supported by the Zoonoses Research Center, Tehran University of Medical Sciences (Grant ID: 1403-4-213-75531). The authors acknowledge the support of the Vice-Chancellorship for Health Affairs, Guilan University of Medical Sciences, and the School of Health, Guilan University of Medical Sciences, for their guidance and assistance during this study. The authors also acknowledge the use of ChatGPT (OpenAI) for language refinement and manuscript editing. All scientific content, interpretations and conclusions remain the sole responsibility of the authors.

https://doi.org/10.18502/jad.v20i2.22399

Ethical consideration

Field sampling of *Aedes albopictus* was conducted by Guilan University of Medical Sciences as part of its routine vector surveillance program. No human participants or vertebrate animals were involved, and no personal or sensitive data were collected. Therefore, additional ethical approval was not required. The ethics approval code for this dissertation is IR.TUMS.REC.1403.215

Conflict of interest statement

The authors declare that there is no conflict of interest.

References

1. Leta S, Beyene TJ, De Clercq EM, Amenu K, Kraemer MU, Revie CW (2018) Global risk mapping for major diseases transmitted by *Aedes aegypti* and *Aedes albopictus*. Int J Infect Dis. 67: 25–35.
2. Grange L, Simon-Loriere E, Sakuntabhai A, Gresh L, Paul R, Harris E (2014) Epidemiological risk factors associated with high global frequency of inapparent dengue virus infections. Front Immunol. 5: 280.
3. Htun TP, Xiong Z, Pang J (2021) Clinical signs and symptoms associated with WHO severe dengue classification: a systematic review and meta-analysis. Emerg Microbes Infect. 10(1): 1116–1128.
4. Akinsulie OC, Idris I (2024) Global re-emergence of dengue fever: The need for a rapid response and surveillance. Microbe. 4: 100107.
5. Yadegarynia D, Keyvanfar A, Keramati A, Najafiarab H, Norouzi S, Soleimani S, Bodaghi A, Arshi S, Tehrani S, Sharafi F, Darvishi A, Moradi G (2025) A national report on 2024 dengue fever outbreak in Iran: has the game changed? BMC Infect Dis. 25(1): 1077.
6. Sedaghat MM (2025) Commentary: Dengue fever: a decade of burden in Iran. Front Public Health. 13: 1553489.
7. Bagherzadeh F, Hemati S, Mohammadi-Moghadam F, Sanami S, Salehifard A, Ahmad S, Farhadkhani M (2025) Environmental Determinants of Dengue Fever: A Re-Emerging Threat in the Middle East. Health Sci Rep. 8(8): e71177.
8. Ducheyne E, Tran Minh NN, Haddad N, Bryssinckx W, Buliva E, Simard F, Malik MR, Charlier J, De Waele V, Mahmoud O, Mukhtar M, Bouattour A, Hussain A, Hendrickx G, Roiz D (2018) Current and future distribution of *Aedes aegypti* and *Aedes albopictus* (Diptera: Culicidae) in WHO Eastern Mediterranean Region. Int J Health Geogr. 17(1): 4.
9. Sedaghat MM, Bozorg-Omid F, Karimi M, Haghi S, Hanafi-Bojd AA (2023) Modelling the probability of presence of *Aedes aegypti* and *Aedes albopictus* in Iran until 2070. Asian Pac J Trop Med. 16(1): 16–25.
10. Azari-Hamidian S, Norouzi B, Maleki H, Rezvani SM, Pourgholami M, Oshaghi MA (2024) First record of a medically important vector, the Asian tiger mosquito *Aedes albopictus* (Skuse, 1895) (Diptera: Culicidae), using morphological and molecular data in northern Iran. J Insect Biodivers Syst. 10(4): 953–963.
11. Dhimal M, Gautam I, Joshi HD, O'Hara RB, Ahrens B, Kuch U (2015) Risk factors for the presence of chikungunya and dengue vectors (*Aedes aegypti* and *Aedes albopictus*), their altitudinal distribution and climatic determinants of their abundance in central Nepal. PLoS Negl Trop Dis. 9(3): e0003545.
12. Ramazannejad Y, Zarghamfard M, Hajisharifi A, Azar S (2021) Factors behind tourists' travel motivation: The case of the Gilan region, Iran. Quaest Geogr. 40 (4): 101–112.
13. Majidi A, Mirzapour Al-e-Hashem SM,

Hashemkhani Zolfani S (2021) Sustainability ranking of the Iranian major ports by using MCDM methods. Mathematics. 9(19): 2451.
14. Kheyroddin R, Kamali J, Esfahani NM (2025) Free trade zones as development engines: Anzali's local manufacturing gains, systemic challenges and regional development lessons (Iran). Res Sq. Available at: https://doi.org/10.21203/rs.3.rs-7232727/v1
15. Brady OJ, Johansson MA, Guerra CA, Bhatt S, Golding N, Pigott DM, Delatte H, Grech MG, Leisnham PT, Maciel-de-Freitas R, Styer LM, Smith DL, Scott TW, Gething PW, Hay SI (2013) Modelling adult *Aedes aegypti* and *Aedes albopictus* survival at different temperatures in laboratory and field settings. Parasit Vectors. 6: 351.
16. Reinhold JM, Lazzari CR, Lahondère C (2018) Effects of the environmental temperature on *Aedes aegypti* and *Aedes albopictus* mosquitoes: a review. Insects. 9(4): 158.
17. Prevention ECfD, Control (2017) Vector control with a focus on *Aedes aegypti* and *Aedes albopictus* mosquitoes: literature review and analysis of information. ECDC, Stockholm.
18. Doeurk B, Leng S, Long Z, Maquart P-O, Boyer S (2025) Impact of temperature on survival, development and longevity of *Aedes aegypti* and *Aedes albopictus* (Diptera: Culicidae) in Phnom Penh, Cambodia. Parasit Vectors. 18(1): 362.
19. Vasconcelos RN, Cantillo-Pérez T, Franca Rocha WJS, Aguiar WM, Mendes DT, de Jesus TB, de Santana CO, de Santana MMM, Oliveira RP (2024) Advances and challenges in species ecological niche modeling: A mixed review. Earth. 5(4): 963–989.
20. Phillips SJ, Anderson RP, Schapire RE (2006) Maximum entropy modeling of species geographic distributions. Ecol Modell. 190(3–4): 231–259.
21. Palo SK, Panda PP, Parida D, Malick ST, Pati S (2025) Remote sensing and GIS-based study to predict risk zones for mosquito-borne diseases in Cuttack district, Odisha, India. GeoHealth. 9(6): e2023GH001007.
22. Riahi K, Van Vuuren DP, Kriegler E, Edmonds J, O'neill BC, Fujimori S, Bauer N, Calvin K, Dellink R, Fricko O, Lutz W (2017) The Shared Socioeconomic Pathways and their energy, land use and greenhouse gas emissions implications: An overview. Global Environmental Change. 42: 153–168.
23. Bazin M (2001) GĪLĀN i. Geography and Ethnography. Encyclopædia Iranica. Vol. X, Fasc. 6: 617–625. Available at: https://www.iranicaonline.org/articles/gilan-index/.
24. Iran S (2016) Statistical Centre of Iran. Iran Population and Housing Census. Statistical Centre of Iran, Tehran.
25. Moussakazemi SM, Rahmani M, Hosseini SA, Pourkhodadad B (2024) Urban tourism development strategies with a cultural-historical approach (Case Study: Gilan Province). Geography. 22(81): 51–68.
26. Research Laboratory and Insectarium of Medical Entomology and Vector Control, the Vice-Chancellorship for Health Affairs, Guilan University of Medical Sciences (2024) Entomological survey data on *Aedes albopictus* occurrence in Guilan Province [Unpublished data].
27. Azari-Hamidian S, Harbach RE (2009) Keys to the adult females and fourth-instar larvae of the mosquitoes of Iran (Diptera: Culicidae). Zootaxa. 2078: 1–33.
28. Azari-Hamidian S, Harbach RE (2025) Updated checklist of the mosquitoes (Diptera: Culicidae) known to occur in Iran, with updated keys to the genera, subgenera and species of *Aedes*. Zootaxa. 5636 (1): 102–120.
29. Brown JL (2014) SDM toolbox: a Python-based GIS toolkit for landscape genetic,

https://doi.org/10.18502/jad.v20i2.22399

biogeographic and species distribution model analyses. Methods Ecol Evol. 5 (7): 694–700.
30. Fick SE, Hijmans RJ (2017) WorldClim 2: new 1-km spatial resolution climate surfaces for global land areas. Int J Climatol. 37(12): 4302–4315.
31. Tatem AJ (2017) WorldPop, open data for spatial demography. Sci Data. 4(1): 1–4.
32. Benedict MQ, Levine RS, Hawley WA, Lounibos LP (2007) Spread of the tiger: global risk of invasion by the mosquito *Aedes albopictus*. Vector Borne Zoonotic Dis. 7(1): 76–85.
33. Kraemer MU, Sinka ME, Duda KA, Mylne AQ, Shearer FM, Barker CM, Moore CG, Carvalho RG, Coelho GE, Van Bortel W, Hendrickx G, Schaffner F, Elyazar IR, Teng HJ, Brady OJ, Messina JP, Pigott DM, Scott TW, Smith DL, Wint GR, Golding N, Hay SI (2015) The global distribution of the arbovirus vectors *Aedes aegypti* and *Ae. albopictus*. Elife. 4: e08347.
34. Montgomery MJ, Harwood JF, Yougang AP, Wilson-Bahun TA, Tedjou AN, Keumeni CR, Wondji CS, Kamgang B, Kilpatrick AM (2025) The effects of urbanization, temperature and rainfall on *Aedes aegypti* and *Aedes albopictus* mosquito abundance across a broad latitudinal gradient in Central Africa. Parasit Vectors. 18: 135.
35. Lorenz C, Castro MC, Trindade PMP, Nogueira ML, de Oliveira Lage M, Quintanilha JA, Parra MC, Dibo MR, Fávaro EA, Guirado MM, Chiaravalloti-Neto F (2020) Predicting *Aedes aegypti* infestation using landscape and thermal features. Sci Rep. 10(1): 21688.
36. O'Dell N, Bolling BG, Dacko N, Carr JT, Hambrick B, Chaves LF, McMillan JR (2025) Identifying environmental drivers of *Aedes aegypti* and *Aedes albopictus* abundance in the Dallas-Fort Worth metroplex using Random Forest modeling. J Med Entomol. 62(4): 789–799.
37. Ibáñez-Justicia A, Alcaraz-Hernández JD, van Lammeren R, Koenraadt CJM, Bergsma A, Delucchi L, Rizzoli A, Takken W (2020) Habitat suitability modelling to assess the introductions of *Aedes albopictus* (Diptera: Culicidae) in the Netherlands. Parasit Vectors. 13(1): 217.
38. Wimberly MC, Davis JK, Evans MV, Hess A, Newberry PM, Solano-Asamoah N, Murdock CC (2020) Land cover affects microclimate and temperature suitability for arbovirus transmission in an urban landscape. PLoS Negl Trop Dis. 14(9): e0008614.
39. Obenauer JF, Andrew Joyner T, Harris JB (2017) The importance of human population characteristics in modeling *Aedes aegypti* distributions and assessing risk of mosquito-borne infectious diseases. Trop Med Health. 45: 38.
40. Rahman MS, Ekalaksananan T, Zafar S, Poolphol P, Shipin O, Haque U, Paul R, Rocklöv J, Pientong C, Overgaard HJ (2021) Ecological, social and other environmental determinants of dengue vector abundance in urban and rural areas of Northeastern Thailand. Int J Environ Res Public Health. 18(11): 5971.
41. Jia P, Chen X, Chen J, Lu L, Liu Q, Tan X (2017) How does the dengue vector mosquito *Aedes albopictus* respond to global warming? Parasit Vectors. 10: 140.
42. Georgiades P, Proestos Y, Lelieveld J, Erguler K (2023) Machine learning modeling of *Aedes albopictus* habitat suitability in the 21st century. Insects. 14(5): 447.
43. Waldock J, Chandra NL, Lelieveld J, Proestos Y, Michael E, Christophides G, Parham PE (2013) The role of environmental variables on *Aedes albopictus* biology and chikungunya epidemiology. Pathog Glob Health. 107(5): 224–241.
44. Peel MC, Finlayson BL, McMahon TA (2007) Updated world map of the Köppen-Geiger climate classification. Hydrol Earth Syst Sci. 11(5): 1633–1644.

http://jad.tums.ac.ir
Published Online: June 30, 2026